

DETERMINATION OF THE INTRINSIC ACTIVITY AND EFFECTIVE
DIFFUSIVITY OF AGED COAL LIQUEFACTION CATALYSTS*

H. P. Stephens and F. V. Stohl

Sandia National Laboratories, Albuquerque, NM 87185

INTRODUCTION

Although severe, rapid catalyst deactivation remains a major economic impediment to the production of liquid fuels from coal by direct processing, there have been few quantitative investigations of aged catalyst intrinsic activity and effective diffusivity. This study reports a method for determining these important properties under experimental conditions that accurately model actual conditions for the processing of coal-derived liquids. The power of the technique has been demonstrated by determination of the intrinsic hydrogenation activity and effective diffusivity of catalysts obtained from the Wilsonville, Alabama coal liquefaction test facility. In addition, modeling of the experimental results has conclusively identified the modes of catalyst deactivation.

The values of intrinsic catalyst activity and effective diffusivity reported here are based on kinetic measurements of the catalytic hydrogenation of pyrene. Pyrene was chosen as a chemical probe of these properties because it appears to play a key role (1,2) as a hydrogen transfer agent in coal liquefaction: hydropyrenes are good hydrogen donors; they have low vapor pressures at liquefaction temperatures; and significant amounts are found in liquefaction solvents (3).

From determination of the pyrene hydrogenation rate constants for pairs of experiments, one with powdered catalyst and the other with whole extrudates, the fraction deactivated and the Thiele modulus, which relates the intrinsic rate constant to the extrudate effective diffusivity, were determined. Experiments with fresh, aged and regenerated catalysts have allowed the contribution of deactivation due to metallic contaminants to be separated from that due to carbonaceous material, and thus has allowed the mode of deactivation for each contaminant to be determined.

THEORY OF DIFFUSION AND REACTION OF PYRENE IN CATALYSTS

Pyrene Hydrogenation Kinetics

Although pyrene (Py) is catalytically hydrogenated to several products, under the conditions used in this study the major product is 4,5-dihydroxyrene (H_2Py). Previous work (4,5) has shown that the hydrogenation of pyrene (reaction [1]) can be precisely described by pseudo first order reversible kinetics (equation [2]):



* This work supported by the U. S. Dept. of Energy at Sandia National Laboratories under contract DE-AC04-76DP00789.

$$\ln \frac{X_e}{X_e - X_t} = kt \quad [2]$$

where k is the sum of the forward (k_1) and reverse (k_{-1}) rate constants, and X_t and X_e are the extents of reaction of pyrene to dihydropyrene at time t and equilibrium. X_t is calculated directly from the experimental product distribution:

$$X_t = \frac{[H_2PY]_t}{[PY]_t + [H_2PY]_t} \quad [3]$$

X_e is calculated from the experimentally observed hydrogen pressure p and the pressure equilibrium constant K_p :

$$X_e = \frac{[H_2PY]_e}{[PY]_e + [H_2PY]_e} = \frac{pK_p}{1 + pK_p} \quad [4]$$

where:

$$K_p = \frac{1}{p} \frac{[H_2PY]_e}{[PY]_e} \quad [5]$$

Catalyst Activity and Effective Diffusivity

Fresh Catalysts. For fresh catalyst extrudates, the fraction of the surface area used for chemical reaction is given by the effectiveness factor ϵ , defined as the ratio of the actual reaction rate for the extrudate to the intrinsic reaction rate (i.e., without diffusion resistance). The effectiveness factor may be determined from the intrinsic rate constant (k_i) for experiments with finely powdered catalyst and the apparent rate constant (k_a) for experiments with whole catalyst extrudates

$$\epsilon = \frac{k_a}{k_i} \quad [6]$$

Upon solving the differential equation for simultaneous diffusion and reaction in a catalyst particle (6), it is found that the effectiveness factor is a function of the Thiele modulus, h :

$$\epsilon = \frac{\tanh(h)}{h} \quad [7]$$

The Thiele modulus for catalyst pellets of all shapes may be closely approximated (7) by the following equation:

$$h = \frac{V_p}{S_x} \sqrt{\frac{\rho k_w}{D_e}} \quad [8]$$

where V_p and S_x are the volume and external surface area of the catalyst pellet, ρ is the pellet density, k_w is the intrinsic rate constant on a catalyst weight (w) basis [equal to $(k_1 + k_{-1})/w$ for reversible reactions (6)] and D_e is the effective diffusivity (diffusion coefficient within the catalyst pellet). Because the Thiele modulus can be determined from equation [7] using the effectiveness factor given by equation [6], the effective diffusivity can be readily calculated by rearrangement of equation [8]:

$$D_e = \left(\frac{V_p}{S_x} \right)^2 \left(\frac{1}{h} \right)^2 \rho k_w \quad [9]$$

Aged and Regenerated Catalysts. The relationship of the fraction F of aged pellet activity remaining to the Thiele modulus h and fraction poisoned α is given by the following equations for the limiting cases of uniform and pore mouth poisoning (8):

Uniform poisoning -

$$F = \left[\frac{\tanh(h \sqrt{1 - \alpha})}{\tanh(h)} \right] \sqrt{1 - \alpha} \quad [10]$$

Pore mouth poisoning -

$$F = \left[\frac{\tanh[(1 - \alpha)h]}{\tanh(h)} \right] \left[\frac{1}{1 + \alpha h \tanh[(1 - \alpha)h]} \right] \quad [11]$$

These equations were derived assuming deactivation results only from poisoning. However, coal liquefaction catalysts may deactivate as a result of the combined effects of uniform and pore mouth poisoning, and pore size reduction. We therefore modified equation [11] to include all of these modes of deactivation. The resulting equation models the fraction of pellet activity remaining for an aged catalyst which may have a completely deactivated shell due to pore mouth poisoning, a partially deactivated core due to uniform poisoning and an effective diffusivity which is less than that of the fresh catalyst:

$$F = \left[\frac{\tanh[(1 - \alpha_s)h]}{\tanh(h_f)} \right] \left[\frac{1}{1 + \alpha_s h \tanh[(1 - \alpha_s)h]} \right] \sqrt{\frac{\rho k_c D_e}{\rho_f k_f D_{ef}}} \quad [12]$$

where h_f , ρ_f , k_f and D_{ef} are the Thiele modulus, pellet density, rate constant and effective diffusivity for the fresh catalyst; h , ρ and D_e are the corresponding parameters for the aged catalyst; α_s is the fraction deactivated by shell progressive pore mouth poisoning; and k_c is the rate constant of the partially deactivated catalyst core given by:

$$k_c = (1 - \alpha_c) k_f \quad [13]$$

where α_c is the fraction of the core that is deactivated. Use of equation [12] to calculate effective diffusivities for aged and regenerated catalysts is discussed in the Results Section.

EXPERIMENTAL

Catalysts

Extrudates (0.8 mm diameter by 4 mm long) of Shell 324M, a 12.4% Mo, 2.8% Ni on alumina catalyst used in second-stage processing (9) of liquids derived from Illinois No. 6 (Burning Star) coal were obtained from the Wilsonville, Alabama coal liquefaction test facility. Fresh catalyst samples, used for baseline activity comparisons, were activated by presulfiding for 6 hours at 400°C and atmospheric pressure using a mixture of 10 mole % H₂S in H₂. Aged catalysts consisted of samples periodically withdrawn from the hydroprocessing reactor during run 242. In addition, samples were obtained from runs 242, 243 and 244, following process catalyst presulfiding with dimethyldisulfide in an oil vehicle, but prior to coal-derived liquid processing. Upon receipt, the aged catalysts, which were shipped in toluene, were Soxhlet extracted with tetrahydrofuran (THF) to remove as much of the soluble hydrocarbons as possible, then dried under vacuum at 100°C to remove traces of THF.

To investigate the effect of deactivation by contaminant metals, carbonaceous material was removed from the aged catalysts by slowly heating the extrudates to 500°C in air over a period of several hours and leaving them at this temperature overnight. These regenerated samples were then resulfided by the same method used for presulfiding the fresh catalyst in the laboratory. The baseline catalyst for experiments with these regenerated samples was a fresh catalyst sample which was treated by the same method as the regenerated samples.

All of the aged catalysts were characterized by a number of techniques including quantitative analysis for metals and carbon, BET surface area and desorption pore volume. In addition, the catalyst sample with the greatest age (527 lb SRC/lb catalyst) was subjected to electron microprobe analysis for metals distribution within the catalyst extrudate.

Pyrene Hydrogenation

The techniques used for the catalytic pyrene hydrogenation reactions and subsequent product analyses have been reported in detail elsewhere (4) and are only briefly described here. Batch reactions were performed (at a temperature of 300°C and nominal hydrogen pressure of 525 psia) in stainless steel microreactors loaded with 100 mg of pyrene, 1 g of hexadecane solvent and 15-19 mg of catalyst. The reactors, which could be rapidly heated to reaction temperature and quenched to ambient temperature at the completion of an experiment, were agitated during the heating period.

Several initial experiments were performed to determine the pressure equilibrium constant for hydrogenation of pyrene to 4,5-dihydropyrene at 300°C and to verify that pseudo first order reversible kinetics accu-

rately modeled the rate of reaction. Following these, hydrogenation experiments for all the fresh, aged and regenerated catalysts were performed in pairs, one experiment with catalyst ground to pass through a 200 mesh sieve (particle diameter 75 μm) to eliminate intraparticle diffusion and the other with whole catalyst extrudates (usually 4-5 per reactor). A nominal weight of 15.4 mg was used for the fresh catalyst. The weights of the aged and regenerated catalysts were increased in proportion to their density to compensate for the weight of contaminants.

Reaction times, which ranged from 10 to 120 minutes, were adjusted according to the activity of the catalysts. Following the completion of an experiment, the products were quantitatively removed from the reactor for analysis by gas-liquid chromatography. In order to determine the ratio of extrudate volume to external surface area, each catalyst extrudate was carefully recovered for measurement of the diameter and length.

RESULTS

Catalyst Characterization

Table I lists the results of characterization of the fresh and aged catalysts. As can be seen from Table I, carbon contents increased rapidly during process presulfiding and initial coal-liquids processing, then remained approximately constant after an age of 88 lbs SRC/lb catalyst. However, the amount of contaminant metals, Fe and Ti, continued to increase throughout the run. Catalyst surface areas and pore volumes varied inversely with the carbon contents. Both exhibit a rapid decline during the initial phase of processing followed by nearly constant values after an age of 88 lb SRC/lb catalyst. These trends in amounts of contaminants and physical properties are similar to those found by other investigators of hydroprocessing catalysts (10,11).

Figure 1 shows distribution of the iron and titanium contaminants, determined by electron microprobe analysis, across a circular cross-section of the 527 lb SRC/lb catalyst extrudate (sample 97001). These metals are deposited in an annular shell of the extrudate, a behavior typical of shell progressive pore mouth poisoning.

Figure 2 illustrates the pore volume distribution for fresh Shell 324M and the aged and regenerated 527 lb SRC/lb catalyst sample. As can be seen, the aged catalyst appears to suffer a large loss of pore volume (and related surface area) in the 70 to 140 A diameter pore region. Previous investigators (12,13) have hypothesized that this loss of pore volume and surface area, which is obviously due to the gain in carbon content, is responsible for loss in catalyst activity due to pore blockage with carbonaceous deposits. However, much of the carbonaceous material may simply be trapped reactant and product which is mobile at reaction temperature and does not contribute to pore blockage. Comparison of the curves for the fresh and regenerated catalyst shows that nearly all of the pore volume of the aged catalyst is restored upon removal of the carbonaceous material by regeneration.

Rate Constants

Results of the initial experiments with ground, freshly presulfided catalyst were used to calculate the pressure equilibrium constant, $1.4 \times 10^{-3} \text{ psia}^{-1}$, (equation [5]) for reaction [1] at 300°C. Figure 3, a plot of $\ln(X_e/(X_e - X_t))$ vs time for these experiments, demonstrates that the reaction rate follows pseudo first order kinetics. The slope of the linear fit of the data is $k_1 + k_{-1}$ or k of equation [2]. Because $\ln(X_e/(X_e - X_t))$ varies linearly with time and has an intercept of zero, the rate constant may be calculated from the results of a single experiment:

$$k = \ln(x_e/(x_e - x_t))/t \quad [14]$$

Catalyst Activity and Effective Diffusivity

Fresh Catalyst. The Thiele moduli of the fresh catalysts were calculated from the experimental effectiveness factors ϵ (ratio of rate constant for the extrudate catalyst to that of the ground, equation [6]) by determining the value of h which satisfied equation [7]. The effective diffusivities were calculated using equation [9] where the ratio of the volume to external surface area is calculated from the average extrudate diameter d and length l :

$$\frac{V_p}{S_x} = \frac{ld^2/4}{d^2/2 + ld} \quad [15]$$

Regenerated Catalysts. The fraction of catalyst shell poisoned, α_s was given by the ratio of the rate constant for ground regenerated catalyst k_r to that of the ground fresh catalyst k_f :

$$\alpha_s = 1 - k_r/k_f \quad [16]$$

while the fraction F of extrudate activity remaining is the ratio of regenerated extrudate rate constant k_{re} to that of the fresh, k_{fe} :

$$F = k_{re}/k_{fe} \quad [17]$$

Because electron microprobe analysis showed that the contaminant metals were deposited in an annular shell of aged extrudates, it was assumed that the cores of the regenerated catalysts were contaminant free and had activities equal to that of the fresh catalyst. The behavior of F vs α_s for regenerated catalyst, discussed in the next section, supports this assumption. Effective diffusivities for the regenerated catalysts were determined by finding the value D_e which satisfied equation [12]. Note that because $\alpha_c = 0$ for regenerated catalysts, the value of the k_c in equations [12] and [13] is equal to k_f .

Aged Catalyst. Calculation of the effective diffusivities for the aged catalysts is similar to that for the regenerated catalyst. Equation [12] is again used; however, the rate constant for the partially deactivated core k_c must be determined from rate constant for the ground aged catalyst experiment k_{wa} and α_s for the corresponding regenerated catalyst

$$k_c = k_{wa}/(1 - \alpha_s) \quad [18]$$

The fraction of the core which is deactivated α_c is:

$$\alpha_c = 1 - k_c/k_f \quad [19]$$

and the total fraction deactivated α_T is:

$$\alpha_T = 1 - (k_{wa}/k_f) = \alpha_s + \alpha_c - \alpha_s \alpha_c \quad [20]$$

Table II lists the rate constants for the ground catalyst and extrudate experiments and Table III gives the fraction poisoned (α_s for the regenerated catalysts and α_s , α_c and α_T for the aged catalysts), the fraction F of extrudate activity (compared to fresh extrudate) remaining, the Thiele modulus h, and the effective diffusivity D_e .

DISCUSSION

The results given in Tables II and III can be used to describe the trends in catalyst activity and diffusivity with age and to identify the modes of catalyst deactivation.

Catalyst Activity. Intrinsic catalyst activity, i.e., the activity without diffusion limitations, is given by the rate constants for ground catalyst experiments (Table II). Loss of intrinsic activity is best characterized by the α parameters (Table III). For the regenerated catalysts, the total fraction deactivated, α_T , is equal to that due to the metallic contaminants, α_s . However, the total fraction deactivated for the aged catalysts is related to the fraction deactivated by carbonaceous deposits α_c and that by metals α_s as given by equation [20]. As can be seen by the values of α_c in Table III, carbonaceous contaminants contribute to a loss of intrinsic catalyst activity of up to 80% during process presulfiding (sample 94074) before processing of coal even begins. However, nearly all of this activity can be recovered by laboratory regeneration methods. After processing of coal begins, metallic contaminants add to the loss in activity and these losses cannot be recovered by regeneration.

Effective Diffusivity. Both the aged and regenerated samples show the same trend in the decrease in effective diffusivities (Table III) with catalyst age. After an initial decrease of 50% from a value of 6×10^{-6} cm²/sec/cm³ for fresh catalysts to 3×10^{-6} for catalyst ages greater than 42 lb SRC/lb catalyst, the diffusivity remains relatively constant. Thus, compared to a decrease in intrinsic activity (Table II) of a factor of 30 over the course of the run, a decrease in effective diffusivity of a factor of two appears to have a smaller impact on extrudate activity.

Modes of Deactivation. For the limiting modes of uniform or pore mouth deactivation, equation [12] reduces to equation [10] or [11], respectively. The limiting modes of deactivation may be identified (8) by plotting the fraction of initial extrudate activity remaining after deactivation (F in Table III adjusted by the ratio $\sqrt{\rho_D e / \rho_f D_{ef}}$) vs the fraction of catalyst deactivated (α_T in Table III). Uniform deactivation behavior, due to the deactivation of catalytic sites homogeneously throughout the extrudate is described by equation [10] which depicts a decrease in activity approximately proportional to $\sqrt{1 - \alpha_T}$. Pore mouth deactivation behavior, which results in an annular shell of deactivation, is described by equation [11] and shows a much different behavior. For pore mouth deactivation, the loss in extrudate activity as a function of fraction deactivated is much greater than that of homogeneous poisoning for the same degree of deactivation.

Because the regenerated catalysts contain only the metallic contaminants, a plot of F vs α_s identifies the mode of deactivation by metals. However, the aged catalysts contain both metallic and carbonaceous contaminants. The plot of F vs α_T for the aged catalysts may identify the dominant mode of deactivation by the deactivating materials.

Figure 4 shows a plot of $F/\sqrt{\rho D_e/\rho_f D_{ef}}$ vs α_T for the regenerated (circles) and aged catalysts (squares). The points for the regenerated samples were accurately fit with the limiting progressive shell pore mouth deactivation model, equation [11], using the average of the Thiele moduli, 5.7, for the samples with significant metals contamination. In contrast, the points for the aged samples were accurately fit with the limiting uniform deactivation model, equation [10], using the average sample Thiele modulus of 2.1. Thus, the catalysts were deactivated by two different modes--progressive shell pore mouth deactivation by metallic contaminants and uniform deactivation by carbonaceous materials. Although the pore mouth mode of deactivation by metals is permanent and limits the amount of extrudate reactivity which can be recovered upon regeneration, the dominant mode of deactivation, which occurs rapidly, is a uniform deactivation by carbonaceous material.

REFERENCES

1. F. J. Derbyshire and D. D. Whitehurst, *Fuel* 60, 655 (1981).
2. F. J. Derbyshire, P. Varghese and D. D. Whitehurst, *Fuel* 61, 859 (1982).
3. B. R. Rogers, R. L. Jolly and R. M. Whan, "ITSL Solvent Quality Studies," Proceedings of the Dept. of Energy Integrated Two-Stage Liquefaction Meeting, Albuquerque, NM, October 1982.
4. H. P. Stephens and R. N. Chapman, "The Kinetics of Catalytic Hydrogenation of Pyrene--Implications for Direct Coal Liquefaction Processing," ACS Fuel Division Preprints, 28, No. 5, 161 (1983).
5. H. P. Stephens in "Coal Liquefaction Process Research Quarterly Report for July 1 - September 30, 1983, Sandia National Laboratories, SAND83-2426, p. 15, January 1984.
6. C. G. Hill, Jr., "An Introduction to Chemical Engineering Kinetics and Reactor Design," John Wiley, NY (1977).
7. R. Aris, *Chem. Eng. Sci.*, 6, 262 (1957).
8. A. Wheeler, *Catalysis* 2 (105), edited by P. H. Emmett, Reinhold, NY (1955).
9. A. K. Rao, R. S. Pillai, J. M. Lee and T. W. Johnson, "Recent Advances in Two-Stage Coal Liquefaction at Wilsonville," Proceedings of the 8th Annual EPRI Contractors Conference on Coal Liquefaction, EPRI AP-3366-SR, February 1984.
10. G. J. Stiegel, R. E. Tischer and D. L. Cillo, "Catalyst Testing for Two-Stage Liquefaction," Proceedings of the 8th Annual EPRI Contractors Conference on Coal Liquefaction, EPRI AP-3366-SR, February 1984.
11. R. Galiasso, R. Blanco, C. Gonzales and N. Quinteros, *Fuel* 62, 817 (1983).
12. M. J. Chiou and J. H. Olson, *ACS Symp. Ser.* 23, 1421 (1978).
13. B. D. Prasher, G. A. Gabriel and Y. H. Ma, *Ind. Eng. Chem. Process Des. Dev.* 17, 266 (1978).

Table I. Elemental Analysis, Surface Areas and Pore Volumes for the Fresh and Aged Catalysts

Sample	Age (lb feed/lb catalyst)	Active Metals (Wt %)		Major Contaminants (Wt %)			Surface Area (m ² /g)	Pore Volume (cc/g)
		Mo	Ni	C	Fe	Ti		
Fresh	--	12.4	2.8	0.11	.02	.07	158	0.49
15923	Process Presulfided	NA	NA	2.33	NA	NA	142	0.41
97888	Process Presulfided	NA	NA	4.40	NA	NA	137	0.38
94074	Process Presulfided	10.3	2.3	6.1	.04	.14	135	0.35
94495	43	10.3	2.3	8.2	.14	.14	125	0.32
94811	88	10.0	2.2	9.3	.22	.21	113	0.29
94966	133	10.1	2.4	9.6	.28	.30	108	0.28
96460	381	9.5	2.5	9.2	.67	.46	102	0.27
97001	527	9.7	2.4	9.4	.72	.56	100	0.27

Table II. Weight Basis Rate Constants for Ground Catalyst and Extrudate Experiments

Sample	Age (lb/lb)	Aged Catalyst		Regenerated Catalyst	
		Rate Constants (sec ⁻¹ g ⁻¹ x10 ²)		Rate constants (sec ⁻¹ g ⁻¹ x10 ²)	
		Ground	Extrudate	Ground	Extrudate
Fresh	--	15.9	4.1	17.6	4.7
15923	Process Presulfided	8.9	3.3	17.6	5.0
97888	Process Presulfided	3.4	1.5	17.2	4.3
94074	Process Presulfided	2.3	0.99	16.8	3.8
94495	43	1.6	0.39	13.6	1.3
94811	88	1.2	0.59	12.1	1.7
94966	133	0.88	0.37	11.8	0.98
96460	381	0.49	0.32	7.2	0.85
97001	527	0.49	0.26	5.2	0.45

Table III. Fractions Poisoned, α , Fraction Extrudate Reactivity Remaining, F, Thiele Modulus, h, and Effective Diffusivities, De, for Fresh, Aged, and Regenerated Catalysts.

Sample	Aged Catalysts						Regenerated Catalysts			
	α_T	α_S	α_C	F	h	Dex10 ⁶	α_S	F	h	Dex10 ⁶ *
Fresh	--	--	--	1.0	3.8	5.6	--	1.0	3.7	6.2
15923	.44	.003	.44	.81	2.5	6.7	.003	1.06	3.5	6.3
97888	.77	.02	.77	.39	2.1	4.2	.02	.92	3.8	6.0
94074	.84	.04	.84	.26	2.1	2.9	.04	.80	4.2	5.4
94495	.89	.22	.85	.11	3.1	1.3	.22	.28	5.9	2.6
94811	.92	.30	.88	.16	1.6	3.7	.30	.35	4.6	4.5
94966	.93	.30	.91	.11	1.9	2.0	.30	.22	6.2	2.3
96460	.96	.57	.92	.09	1.3	4.2	.57	.19	5.0	3.4
97001	.96	.68	.88	.08	1.8	2.9	.68	.10	6.9	2.1

*De has units of cm²/sec/cm³.

FIGURE 1. Distribution of Fe and Ti across a circular cross-section of extrudate sample 97001, aged 527 lbs SRC/lb catalyst.

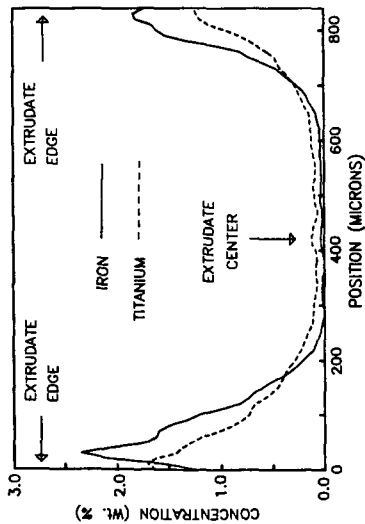


FIGURE 2. Pore volume distribution for fresh catalyst, aged, and regenerated sample 97001.

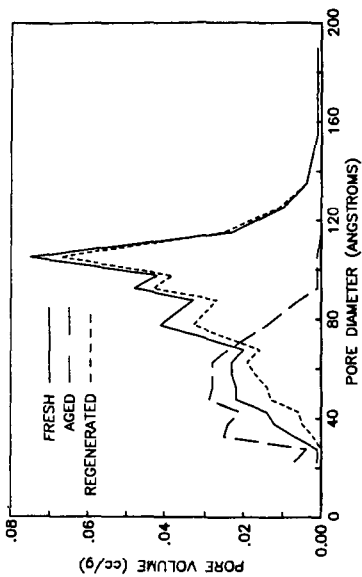


FIGURE 3. Plot of pseudo first order reversible reaction kinetics for hydrogenation of pyrene to 4,5-dihydropyrene.

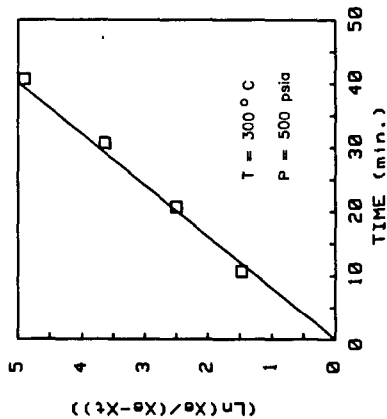


FIGURE 4. Plot of fraction extrudate activity remaining vs total fraction deactivated for aged and regenerated extrudates.

